High Energy Density Physics 23 (2017) 212–216

Contents lists available at ScienceDirect

High Energy Density Physics

journal homepage: www.elsevier.com/locate/hedp

# Robustness of raman plasma amplifiers and their potential for attosecond pulse generation

James D. Sadler[a,*], Marcin Sliwa[a], Thomas Miller[a], Muhammad F. Kasim[a], Naren Ratan[a], Luke Ceurvorst[a], Alex Savin[a], Ramy Aboushelbaya[a], Peter A. Norreys[a], Dan Haberberger[b], Andrew S. Davies[b], Sara Bucht[b], Dustin H. Froula[b], Jorge Vieira[c], Ricardo A. Fonseca[c], Luís O. Silva[c], Robert Bingham[d], Kevin Glize[d], Raoul M.G.M. Trines[d]

[a] Clarendon Laboratory, University of Oxford, Parks Road, Oxford, OX1 3PU, UK
[b] Laboratory for Laser Energetics, 250 East River Road, Rochester, NY 14623, USA
[c] GoLP/Instituto de Plasmas e Fusão Nuclear, Instituto Superior Técnico, Universidade de Lisboa, Lisbon, Portugal
[d] Central Laser Facility, STFC Rutherford Appleton Laboratory, Didcot, OX11 0QX, UK

ARTICLE INFO

*Article History:*
Received 11 May 2017
Accepted 14 May 2017
Available online 15 May 2017

*Keywords:*
Raman scattering
Laser plasma interactions

ABSTRACT

Raman back-scatter from an under-dense plasma can be used to compress laser pulses, as shown by several previous experiments in the optical regime. A short seed pulse counter-propagates with a longer pump pulse and energy is transferred to the shorter pulse via stimulated Raman scattering. The robustness of the scheme to non-ideal plasma density conditions is demonstrated through particle-in-cell simulations. The scale invariance of the scheme ensures that compression of XUV pulses from a free electron laser is also possible, as demonstrated by further simulations. The output is as short as 300 as, with energy typical of fourth generation sources.



## 1. Introduction

Reaching high power and high brightness laser pulses is a primary goal for high energy density science, both for producing and diagnosing extreme plasma conditions. High power pulses across a wide spectral range have a myriad of applications in inertial confinement fusion [1], atomic physics [2], laser particle acceleration [3] and generating matter-antimatter plasmas [4]. Currently chirped pulse amplification using solid state grating compressors is the highest power method in the near optical range, however free electron lasers have also reached unprecedented brightness deep in to the X-ray spectrum. Both suffer the drawback of requiring large scale infrastructure with continuing replacement, limiting the proliferation and maximal power of such sources.

Non-linear optics effects in crystals can also be used to amplify ultra-short pulses, however these are still subject to the same intensity and fluence limitations and still require a grating compressor. Plasma amplifiers circumvent this problem by utilising parametric instabilities in a plasma, a medium that is both compact and cheap. If conditions can be sufficiently controlled, the Raman backscatter instability can be used to compress a long laser pulse (frequency $\omega$), while minimising the growth of other detrimental instabilities [5,6].

To stimulate Raman scattering an electron plasma wave must be resonantly excited, requiring two separate laser pulses differing in frequency by the plasma frequency $\omega_p = \omega\sqrt{n/n_{crit}}$, where $n$ is the electron number density and $n_{crit} = \frac{1.1\times10^{21}}{\lambda_{\mu m}^2}/\mathrm{cm}^3$ is the critical density. The beating of these pulses ponderomotively excites a highly nonlinear plasma wave, and the growth rate is maximised for counter-propagation. The higher frequency long pulse is then scattered by the density perturbation to amplify the shorter, lower frequency pulse. Providing the electron plasma wave is not heavily damped or turbulent, this mechanism can fully deplete the long pump pulse and transfer energy to the shorter pulse at high efficiency. Large scale particle-in-cell and Vlasov simulations [7–10] agree with the analytical result in the non-linear regime, predicting energy transfer from the long to the short pulse greater than 50%.

However, several conditions must be met to preserve the plasma wave fidelity; its small wavelength of approximately half that of the pump pulse makes it delicate [11]. Firstly, it must not be excessively Landau damped, requiring $k\lambda_D < 1$ where $k \simeq (2\omega - \omega_p)/c$ is the wave-number of the Langmuir wave and $\lambda_D$ is the Debye length [12].

A further problem is breaking of the plasma wave, subsequently becoming turbulent and losing coherence. This is a problem due to

* Corresponding author.
*E-mail address:* james.sadler@physics.ox.ac.uk (J.D. Sadler).

http://dx.doi.org/10.1016/j.hedp.2017.05.007

the low phase velocity of the wave. If the wave amplitude is ponderomotively over-driven, electrons will exceed the phase velocity and become trapped. For a cold plasma this occurs for pump pulse dimensionless amplitudes above $0.35(n/n_{crit})^{0.75}$ and worsens for hotter plasmas [9,13–15].

In denser plasmas, collisional damping also plays a significant role if the electron ion collision time is of the order $\omega_p$. Unfortunately the conditions to minimise this problem, low density and high temperature, are the opposite to those minimising Landau damping.

The scheme is also reliant on the three wave resonance, indicating that a chirp in the long pulse or plasma density gradients may decrease performance. Here we show, using particle-in-cell simulations, that the scheme is robust to typical variations.

## 2. Robustness of raman amplifiers to experimental perturbations

Many previous simulations of plasma amplifiers have used uniform plasma density, transform limited Gaussian laser pulses and sometimes even cold, fully ionised plasma. Because Raman backscatter is a resonant process, deviations from these ideal conditions may lead to efficiency losses due to loss of resonance [16], increased kinetic effects or enhanced seeding of competing instabilities [17]. It is an important consideration for any experimental design to know the relevant tolerance for each deviation from these ideal conditions [18–22]. We show here that the non-linear stage (and to a certain extent the linear stage) of the amplification is tolerant to variations in plasma density.

*Variation of Electron Density*

For near optical laser pulses, a typical electron density of $n/n_{crit} \simeq 0.01$ requires a gas target of approximately atmospheric pressure for hydrogen. A typical experimental target will use a room temperature gas system, requiring a gas burst in to the vacuum chamber shortly before the laser pulse arrival. This means the neutral gas is often in a transient hydrodynamic state before the interaction and therefore the electron number density $n_e$ is hard to predict or control, and may not be spatially uniform. This can be countered, with considerable complexity, by using low density solid targets or cryogenic liquefied gasses.

However, a gaseous target may be sufficient if the Raman amplification is robust to density variations in the target. Changes in plasma density could cause a loss of resonance with the plasma wave. However, theory indicates that the amplification has a wide bandwidth in the non-linear stage and may withstand the slight deviation from perfect resonance.

The high efficiency non-linear stage requires that the seed pulse meets the condition [23]

$$a_{seed} T \sqrt{\omega \omega_p} = 5, \tag{1}$$

where $a_{seed}$ and $T$ are the seed pulse peak dimensionless amplitude and full width at half maximum duration of the seed intensity envelope. For linear polarisation, the amplitude is related to the pulse intensity and wavelength through $I = 1.4 \times 10^{18} a_{seed}^2 / \lambda_{\mu m}^2$, with units W/cm$^2$ and microns. The pump pulse amplitude can also be found in this way. This is an attractive solution, so it continues to hold throughout the non-linear amplification stage.

Assuming this condition is met, we may estimate the maximum tolerable plasma density variations by first evaluating the seed pulse bandwidth in the non-linear stage. Assuming the seed is a transform limited Gaussian with duration given by (1), we find the full width at half maximum bandwidth of the spectral power is

$$\Delta\omega_{seed}/\omega = \frac{4\ln(2) a_{seed}}{5} \sqrt{\frac{\omega_p}{\omega}}. \tag{2}$$

As a basic model, any changes in plasma density must not move the resonance outside of the bandwidth of the seed pulse, therefore the maximum tolerable density variation in the non-linear stage is

$$\frac{\delta n}{n} = 2\frac{\delta\omega_p}{\omega_p} = -2\frac{\delta\omega}{\omega_p} = -2\frac{\delta\omega_{seed}}{\omega}\frac{\omega}{\omega_p} = \frac{a_{seed}}{2}\sqrt{\frac{\omega}{\omega_p}}. \tag{3}$$

Where we have used the result (2) and assumed the seed pulse satisfies the non-linear solution (1). For a seed amplitude of 0.1 in the nonlinear stage and density $n_0/n_{crit} = 0.01$, as simulated, this gives a density tolerance of 16%. This is a large value and easily achievable experimentally. The tolerance increases as the pulse amplifies through the nonlinear stage.

To verify the expression (3), we conducted a series of one-dimensional Particle-in-Cell simulations where the transform limited seed pulse is initialised on the non-linear solution (1) with central frequency $\omega_{seed} = 0.9\omega$. The pump amplitude was constant at 0.01, with a uniform plasma of variable density. The electron temperature was 50 eV. The seed was initialised on the nonlinear trajectory (Eq. 1) with dimensionless amplitude 0.1. The energy transfer efficiency after a 300 wavelength propagation is shown in Fig. 1. The box length was $200\lambda_0$ and it moved with the amplified pulse. There were 128 particles per cell and 120 cells per pump wavelength. Efficiency was calculated by first subtracting the pump pulse, finding the change in fluence from the initial seed, then dividing by the total fluence of the pump pulse.

There is clearly great resilience to de-tuning for the pulse in the nonlinear stage, so experimental density variations will be of little concern. The tolerance to density de-tuning agrees with the estimate of 16%. The expected resonant density is $n/n_{crit} = (1-\omega_{seed}/\omega)^2 = 0.01$. The maximal efficiency is found for a density slightly higher than this. This is due increased kinetic effects at lower densities.

The growth in the linear stage is likely to be more susceptible to de-tuning as the linear Raman instability has a narrow bandwidth. However, if the seed pulse bandwidth is greater than this then there will still be a good tolerance. The simulations were repeated for an identical transform limited seed pulse but with peak amplitude 0.01, far below the non-linear stage. The tolerance, also shown in Fig. 1a, is similar to the previous case because the seed bandwidth is the same. A wide bandwidth seed pulse is therefore an effective strategy to increase the tolerance to plasma variations.

The maximal efficiency occurs for a density slightly less than $0.01 n_{crit}$. This is because kinetic effects are less important for this lower seed intensity and the plasma wave frequency is slightly increased by its temperature dependence.

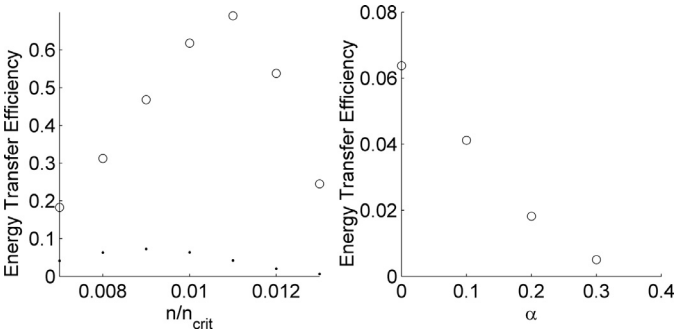


**Fig. 1.** Investigation of the effects of density variations. (a) Energy transfer efficiency after a 300 wavelength propagation is shown versus the uniform plasma density. The open circles are for $a_{seed} = 0.1$ and the dots for $a_{seed} = 0.01$, both with transform limited duration $22\lambda$. The seed frequency was 0.9 of the pump frequency. The amplifier is largely unaffected by variations up to 20%, due to the wide bandwidth of the seed pulse. (b) Effects of a linear density gradient for the $a_{seed} = 0.01$ case. $\alpha$ is the density change, as a fraction of the starting density, over the 300 wavelength propagation.

In the linear stage, the Raman back-scatter is likely to have a narrower bandwidth than the seed pulse. This means a density gradient could move the resonance away from this spectral peak and prevent exponential growth. To investigate this separate effect, further simulations initialised a density gradient.

Fig. 1b shows a repeat of the $n_0 = 0.01 n_{crit}$ case, now with a linear density gradient $n/n_0 = 1 + \alpha x/(300\lambda)$ and $a_{seed} = 0.01$. The efficiency after propagating 300 wavelengths is shown versus $\alpha$.

De-tuning the density in this way has previously been suggested as a method to reduce growth of Raman forward scatter, as the amplified pulse is more resistant due to its wider bandwidth. This strong growth even with a plasma density gradient was previously predicted [24–27] and now observed in these simulations, up to a limit broadly agreeing with the result (3).

As well as loss of resonance, spatial variations in the plasma density could seed competing instabilities, particularly ponderomotive filamentation of the amplified pulse. This additional effect was investigated with a two dimensional simulation. The plasma was assumed pre-ionised, with an artificial density variation, initialised as a Fourier series in two spatial dimensions:

$$n_e(\mathbf{x})/n_0 = 1 + 0.01 \sum_{j=1}^{10} \sin(2\pi j \mathbf{k_j}.\mathbf{x}/L) \quad (4)$$

Here the $\mathbf{k_j}$ vectors are randomly directed unit vectors and $L$ is the simulation box width. The average density $n_0$ is kept as $0.01 n_{crit}$. This gives forwards and transverse components to the density modulation and a peak amplitude of 10%, with modes from the full box width down to the plasma wavelength. The simulation used a domain moving along with the amplified pulse, of length $125\lambda_{pump}$ and width $100\lambda_{pump}$. To reflect realistic experimental conditions, the plasma was initialised with electron temperature 50 eV and the initial seed pulse parameters were well below the requirement (1) for the high efficiency behaviour.

The Gaussian seed pulse had peak amplitude 0.01, frequency $0.9\omega_{pump}$ and duration $22\lambda_{seed}/c$. The pump pulse had constant amplitude 0.02. Both pulses had plane wave transverse profiles, aligned linear polarisation, periodic boundary conditions transversely and absorbing at the rear of the moving window. Cell dimensions were $\lambda_{pump}/60$ by $\lambda_{pump}/5$, each with 36 electron particles. Ions were kept as a static neutralising background.

Fig. 2b shows the final intensity profile after a propagation of $2400\lambda_{seed}$. The density perturbations have led to minor filamentation. Fig. 2c shows the complex phase of the Fourier transform of the amplified pulse, demonstrating that the plasma amplifier introduces a relative phase difference of much less than $\pi$ across the full aperture. Comparison to the case with uniform plasma shows that the filament amplitude is only slightly worsened by the presence of density perturbations on the 5–10% level. The dominant filament mode is on the scale of the plasma wavelength. This is an important result for subsequent focusing of the amplified pulse, as transverse coherence is largely retained even with non-ideal conditions over thousands of wavelengths.

*Variation of Laser Phase Profile*

Variations in the phase profile of the pump pulse may also have an effect similar to a plasma density gradient. Typical experimental values are $\delta\omega/\omega \simeq 10^{-3} - 10^{-2}$. A one-dimensional simulation was used to investigate the effect of frequency chirp on the pump pulse, for typical experimental conditions. Low intensity spontaneous back-scatter could be more strongly affected than the amplified seed pulse, due to its lower bandwidth [24,28]. This could have the beneficial effect of improving the pulse contrast.

Since $\delta\omega_{seed} = -\delta\omega_{pump}$, the maximum pump pulse chirp before the process is detuned is also given by Eq. 2. The bandwidth of a typical pump pulse is within this value. It was confirmed by a further simulation that there was little to no effect to the uniform plasma simulation in Fig. 1b when a typical pump bandwidth of $\Delta\omega/\omega = 0.002$ was included by chirping the pump pulse.

## 3. Summary of attosecond XUV pulse generation

The fledgling field of ultra-fast science, resolving evolution timescales down to attoseconds ($10^{-18}$s), aims to probe atomic processes important in chemical reactions and resolve the motion of electrons bound in atoms. The resulting advances are applicable to many fields including biochemistry, semiconductors and atomic physics. There are currently several techniques for generating attosecond pulses through high harmonic generation [29] and innovative schemes with X-ray free electron lasers (XFEL) [30].

However, the pulse fluence must be improved to act as an effective probe pulse. Raman back-scatter from an X-ray free electron laser pulse, in an under-dense plasma, may be used to achieve this. A short seed pulse from a high harmonic source, such as those generated in reference [31], may be amplified using an XFEL pump pulse. For XUV pulses with wavelength 10 nm, the required plasma density

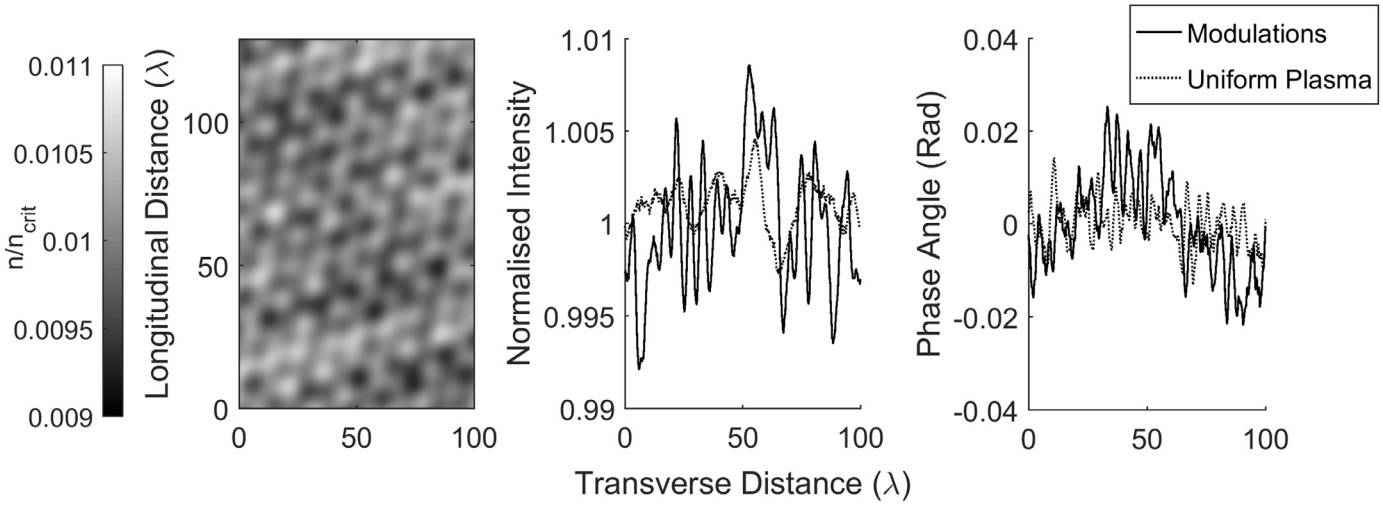


**Fig. 2.** Effects of density variations in two dimensions. The simulation initialised plasma density modulations with a variety of spatial modes. (a) The 2D spatial density modulations initialised in the simulation. (b) The final intensity of the amplified pulse across its transverse dimension, at the position of peak intensity. (c) The complex phase of the Fourier transform of the amplified pulse electric field at $k = 2\pi/\lambda_{seed}$. Both line-outs are compared to an equivalent simulation with uniform plasma at the mean density.

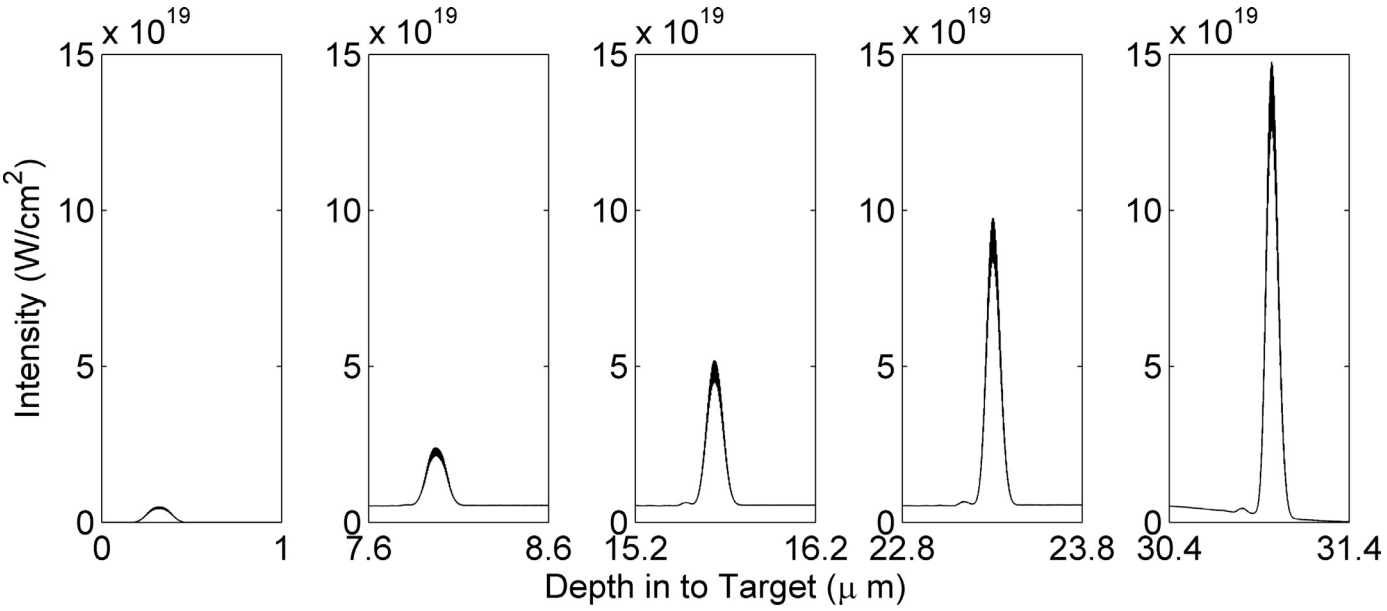


**Fig. 3.** Amplification of a 10 nm wavelength high harmonic seed pulse in a static window particle-in-cell simulation. The intensity of the amplified pulse is shown at five time-steps (each separated by 26 fs) within the 30 $\mu$m plastic target, fully ionised and expanded by a pre-pulse to a constant density of $5.5 \times 10^{22}/\text{cm}^3$. The counter-propagating XFEL pulse was modelled at constant intensity. The simulation included a binary collision routine, with collisional absorption raising the temperature to 500 eV over the full simulation.

is around $10^{22}/\text{cm}^3$. For shorter wavelength X-rays, collisional or Landau damping are significant and prohibitively reduce energy transfer [32,33]. The temperature must be high enough for a weakly coupled plasma, but not so high that the wave is Landau damped. Since $n\lambda_D^3 \simeq 50$, particle-in-cell simulations can effectively model these conditions, providing the collisional damping is well modelled with a binary collision routine.

A range of plasma densities were modelled using the particle-in-cell code OSIRIS. Simulations used a long pump of constant amplitude $a_0 \simeq 0.01$, within achievable limits using X-ray optics to focus an XFEL pulse. Although performance is reduced by the various damping effects, a total energy transfer of 8% was found for optimal plasma density and temperature [34]. The resulting pulses had duration as low as 300 as, over an order of magnitude shorter than currently achieved with free electron lasers (Fig. 3).

The optimal plasma density was $5 \times 10^{22}/\text{cm}^3$, approximately 1/10 of solid density. A free electron laser pulse of 250 fs duration requires a 40 $\mu$m thickness plasma target. This could be generated from a 4 $\mu$m plastic foil, expanded and heated by an optical pre-pulse. A suitable seed pulse could be generated from a separate high harmonic source such as routinely delivered at facilities such as Artemis at the Central Laser Facility [35].

As previously predicted [32,36], the simulated performance is degraded for wavelengths in to the hard X-ray spectrum. This is due to excessive atomic and collisional absorption and the lower seed energy for high harmonics deeper in to the X-ray spectrum. This could potentially be countered, with greater complexity, by a second free electron laser acting as a seed.

A proof of concept experiment is feasible, especially considering recent addition of petawatt sources to X-ray free electron laser facilities. High harmonics from a petawatt solid target interaction could also act as an effective seed. The requirements are a pre-heating beam, a high harmonic source and a soft X-ray free electron laser. High harmonic sources lead to a train of pulses, each of which could be amplified by the plasma Raman back-scatter, possibly providing a train of energetic attosecond pulses separated by several femtoseconds. Such a tool would be invaluable for probing ultra-fast processes.

## Acknowledgements

This work has been carried out within the framework of the EUROfusion Consortium and has received funding from the Euratom research and training programme 2014–2018 under grant agreement No 633053. This work has also been funded by EPSRC grant number EP/L000237/1 and by STFC grant number ST/M007375/1. This work was also supported by the U.S. Department of Energy, Office of Fusion Energy Sciences Award No. DE-SC-0016253. The authors would like to thank the staff of the Central Laser Facility and Scientific Computing Department at STFC Rutherford Appleton Laboratory. This work used the ARCHER UK National Supercomputing Service (http://www.archer.ac.uk) and STFC's SCARF cluster. The authors would like to thank the UCLA/IST consortium for the use of Osiris.

## References

[1] M. Tabak, J. Hammer, M.E. Glinsky, et al., Phys. Plasmas 1 (1994) 1626.
[2] O. Ciricosta, S. Vinko, H.-K. Chung, et al., Phys. Rev. Lett. 109 (2012) 065002.
[3] C. Clayton, J. Ralph, F. Albert, et al., Phys. Rev. Lett. 105 (2010) 105003.
[4] M.R. Edwards, N.J. Fisch, J.M. Mikhailova, Phys. Rev. Lett. 116 (2016) 015004.
[5] V. Malkin, G. Shvets, N. Fisch, et al., Phys. Rev. Lett. 82 (1999) 4448.
[6] R. Trines, F. Fiúza, R. Bingham, et al., Phys. Rev. Lett. 107 (2011) 105002.
[7] R. Trines, F. Fiuza, R. Bingham, et al., Nat. Phys. 7 (2011) 87.
[8] T.-L. Wang, D. Clark, D. Strozzi, et al., Phys. Plasmas 17 (2010) 023109.
[9] M.R. Edwards, Z. Toroker, J.M. Mikhailova, et al., Phys. Plasmas 22 (2015) 074501.
[10] J. Sadler, et al., Phys. Rev. E (accepted, 2017).
[11] D.S. Clark, N.J. Fisch, Phys. Plasmas 10 (2003) 3363.
[12] N. Yampolsky, N. Fisch, Phys. Plasmas 16 (2009) 072105.
[13] J.M. Dawson, Phys. Rev. 113 (1959) 383.
[14] N.A. Yampolsky, N.J. Fisch, Phys. Plasmas 18 (2011) 056711.
[15] J. Farmer, B. Ersfeld, D. Jaroszynski, Phys. Plasmas 17 (2010) 113301.
[16] I. Barth, Z. Toroker, A.A. Balakin, et al., Phys. Rev. E 93 (2016) 063210.
[17] D. Turnbull, S. Li, A. Morozov, et al., Phys. Plasmas 19 (2012) 083109.
[18] J. Ren, W. Cheng, S. Li, et al., Nat. Phys. 3 (2007) 732.
[19] Y. Ping, W. Cheng, S. Suckewer, et al., Phys. Rev. Lett. 92 (2004) 175007.
[20] G. Vieux, A. Lyachev, X. Yang, et al., New J. of Phys. 13 (2011) 063042.
[21] W. Cheng, Y. Avitzour, Y. Ping, et al., Phys. Rev. Lett. 94 (2005) 045003.
[22] N. Yampolsky, N. Fisch, V. Malkin, et al., Phys. Plasmas 15 (2008) 113104.
[23] R. Trines, et al., 2017. https://arxiv.org/abs/1611.04485.
[24] V. Malkin, G. Shvets, N. Fisch, Phys. Rev. Lett. 84 (2000) 1208.
[25] Y.A. Tsidulko, V.M. Malkin, N.J. Fisch, Phys. Rev. Lett. 88 (2002) 235004.
[26] V. Malkin, N. Fisch, Eu. Phys. J. Spec. Top. 223 (2014) 1157.
[27] B. Ersfeld, D. Jaroszynski, Phys. Rev. Lett. 95 (2005) 165002.

[28] Z. Toroker, V. Malkin, N. Fisch, Phys. Rev. Lett. 109 (2012) 085003.
[29] S. Gordienko, A. Pukhov, O. Shorokhov, et al., Phys. Rev. Lett. 94 (2005) 103903.
[30] P. Emma, K. Bane, M. Cornacchia, et al., Phys. Rev. Lett. 92 (2004) 074801.
[31] B. Dromey, M. Zepf, A. Gopal, et al., Nat. Phys. 2 (2006) 456.
[32] V. Malkin, N. Fisch, J. Wurtele, Phys. Rev. E 75 (2007) 026404.
[33] V. Malkin, N. Fisch, Phys. Rev. E 80 (2009) 046409.
[34] J.D. Sadler, R. Nathvani, P. Oleśkiewicz, et al., Sci. Rep. 5 (2015).
[35] I.E. Turcu, E. Springate, C.A. Froud, et al., ROMOPTO 2009, 2009, pp. 746902–746903. International Society for Optics and Photonics
[36] V. Malkin, N. Fisch, Phys. Plasmas 17 (2010) 073109.